Deghosting and its Effect on Noise

Vrolijk, Jan-Willem; Blacquière, Gerrit

DOI
10.3997/2214-4609.201701400

Publication date
2017

Document Version
Final published version

Published in
79th EAGE Conference and Exhibition 2017

We P5 12

Deghosting and its Effect on Noise

J.-W. Vrolijk* (Delft University of Technology), G.J. Blacquière (Delft University of Technology)

Summary

In marine seismic the ghost wavefield results in deep notches in the broadband frequency spectrum corresponding to the depth of the sources and detectors with respect to the sea surface. An inverse filter is used to remove these ghost effects. Application this filter has the consequence that the notch areas are amplified. In the presence of noise, the signal as well as the noise are amplified, which can lead to an unfavourable signal-to-noise ratio. Three methods are compared with respect to signal reconstruction and effect on noise. The first method, the non-causal method is exact for the signal outside the notches and inside the notch areas the noise is controlled with a ceiling applied to the inverse filter. The second method minimizes an objective function in order to indirectly calculate the ghost-free result without explicitly using the inverse filter. Finally, the hybrid method is a combination of these two. The methods are separately applied to a shot with and without noise. In order to quantify which method is most suited with respect to both signal reconstruction and noise suppression, a quantitative analysis is carried out. A constrained closed-loop method is the most accurate for this particular case.

Introduction

In addition to the direct wavefield, a so-called ghost wavefield, generated by a strong sea surface reflectivity, is measured in marine seismic. This ghost wavefield results in deep notches in the wavenumber-frequency domain, their position depends on the depth of the sources and detectors with respect to the sea surface. An inverse filter can be used to remove the ghost effects, consequently the notch areas are amplified. In the presence of noise, the signal as well as the noise is amplified, which can lead to an unfavourable signal-to-noise ratio (SNR). In this abstract a non-causal, closed-loop and hybrid deghosting method are compared with respect to signal reconstruction as well as suppression of noise.

Theory

In marine acquisition, detectors are towed at depth z_d, which spatially can vary. The water surface reflectivity is very strong, which means that at the detector side two wavefields are measured: the first is travelling up from the subsurface, the second is travelling up from the subsurface, getting reflected at the sea surface and then travelling down. In the frequency domain, the forward model for the ghost model becomes:

$$\mathbf{G}^{\cap}(z_d, z_d) = [\mathbf{I} + \mathbf{W}^{+}(z_d, z_0)\mathbf{R}^{\cap}(z_0, z_0)\mathbf{W}^{-}(z_0, z_d)], \tag{1}$$

according to the matrix notation given by Berkhout (1985). Here $\mathbf{W}^{-}$ describes wave propagation from z_d to the sea surface z_0, $\mathbf{W}^{+}$ describes wave propagation from z_0 to z_d , $\mathbf{R}^{\cap}$ is the sea surface reflectivity and $\mathbf{I}$ is the identity matrix. In practice, $\mathbf{R}^{\cap}$ is angle and frequency dependent (Orji et al., 2013). The ghost model at the source side is similar. In this abstract the focus is on the detector side.
The model for seismic data including the detector ghost becomes:

$$\mathbf{P}(z_d) = \mathbf{G}^{\cap}(z_d, z_d)\mathbf{P}_0(z_d), \tag{2}$$

with $\mathbf{P}$ the measured wavefield at the detector level including the ghost, and $\mathbf{P}_0$ is the ghost-free wavefield at z_d. In order to estimate $\mathbf{P}_0$ from $\mathbf{P}$, the inverse ghost filter $[\mathbf{G}^{\cap}(z_d, z_d)]^{-1}$ must be applied to equation 2. As a result from a strong sea surface reflectivity $\mathbf{R}^{\cap}$ deep notches are present in the spectrum. The frequency of the notch area is related to:

$$f_{notch} = \frac{nc}{2z_d} \qquad \text{with} \quad n \in \mathbb{N}, \tag{3}$$

for horizontal wavenumber $k_x = 0$, with c the speed of sound of water and n the order of the notch. If $\mathbf{R}^{\cap} = -\mathbf{I}$ the denominator of the inverse ghost operator will have zeros and therefore becomes unstable. In addition, noise inside the notch areas is amplified by applying the inverse operator $[\mathbf{G}^{\cap}(z_d, z_d)]^{-1}$ resulting in a detrimental SNR. Two different methods are discussed that control the noise during the deghosting procedure.

Non-causal Deghosting

The first method, introduced by Berkhout and Blacquière (2016), describes the non-causal approach:

$$[\hat{\mathbf{G}}^{\cap}(z_d, z_d)]^{-1} = \left[[\mathbf{G}^{\cap}(z_d, z_d)]^{H}\mathbf{G}^{\cap}(z_d, z_d)\right]^{-1}\mathbf{G}^{\cap}(z_d, z_d)]^{H} \tag{4a}$$

for $||\mathbf{G}^{\cap}|| \leq ceiling$, i.e., outside the notch areas, and

$$[\hat{\mathbf{G}}^{\cap}(z_d, z_d)]^{-1} \approx ceiling\ [\mathbf{G}^{\cap}(z_d, z_d)]^{H} \tag{4b}$$

for $||\mathbf{G}^{\cap}|| > ceiling$, i.e., inside the notch areas.

In equation 4 *ceiling* is the maximum amplitude correction, superscript H denotes the conjugate transpose, and the hat symbol ˆ indicates an estimate. Application of the term $[\mathbf{G}^{\cap}]^{H}$ in equation 4 is called 'zero-phasing by correlation'. The zero-phasing step guarantees that the phase of the result is accurate both inside and outside the notch areas. The amplitude correction however, is different inside the notch areas from outside the notch areas. The inversion of the signal outside the notch areas is exact. Inside the notch areas the amplitude correction is limited by the *ceiling* to control noise.

Closed-loop Deghosting

The next method to obtain the ghost-free data is based on minimizing an objective function. We consider three variations. The first one we call 'closed-loop deghosting':

$$J = ||\mathbf{P}(z_d) - \mathbf{G}^{\cap}(z_d, z_d)\mathbf{P}_0(z_d)||^2. \tag{5}$$

In Rickett et al. (2014) a similar objective function is described in the Radon domain including the ghost delay times and an L1 norm to constrain these travel times. In order to suppress the noise more accurately an L1 norm can be added to equation 5, where $\mathbf{p}_0$ is the ghost free data in the time domain:

$$J = ||\mathbf{P}(z_d) - \mathbf{G}^{\cap}(z_d, z_d)\mathbf{P}_0(z_d)||^2 + \lambda|\mathbf{p}_0(z_d)|. \tag{6a}$$

Here the degree of sparsity is controlled with user-defined constant λ which optimal value depends on the SNR. The method is called 'sparse closed-loop deghosting', and can be further stabilized as follows:

$$J = ||\mathbf{P}(z_d) - \mathbf{G}^{\cap}(z_d, z_d)\mathbf{P}_0(z_d)||^2 + \frac{1}{2}\lambda\sqrt{1 + \frac{\mathbf{p}_0^2}{\varepsilon^2}}. \tag{6b}$$

This stabilized L1-L2 norm combines the L2 norm (minimizing total energy) and L1 norm and is stabilized with a constant ε in the order of 0.1%. We call it 'stabilized sparse closed-loop deghosting'. A conjugate gradient method is used to solve equations 5, 6a and 6b to determine $\mathbf{P}_0$ without explicitly calculating $[\mathbf{G}^{\cap}(z_d, z_d)]^{-1}$. At each iteration, events that are present prior to the first arrival are muted to improve convergence.

Example

The effects of the non-causal deghosting, the closed-loop methods, as well as a hybrid method are demonstrated on a single shot record. The hybrid method combines the non-causal method outside the notches with the 'sparse closed-loop' method inside the notch area. The record is generated from the Marmousi model, using an acoustic finite-difference scheme. The spatial detector sampling is 5 m, the time sampling is 4 ms and detectors are located 20 m below the sea surface. As a reference, the ghost-free record is shown in Figure 1a, with its f-k spectrum in Figure 1b. The forward ghost model is applied and gaussian noise is added after the first arrival to get a SNR of 11 dB (Figures 1c and 1d). The notch frequencies appear at 0 Hz, 37.5 Hz and 75 Hz (Figure 1d), which correspond to the values given by equation 3 for detectors at 20 m depth. The source is at zero depth, therefore no source ghost is present.

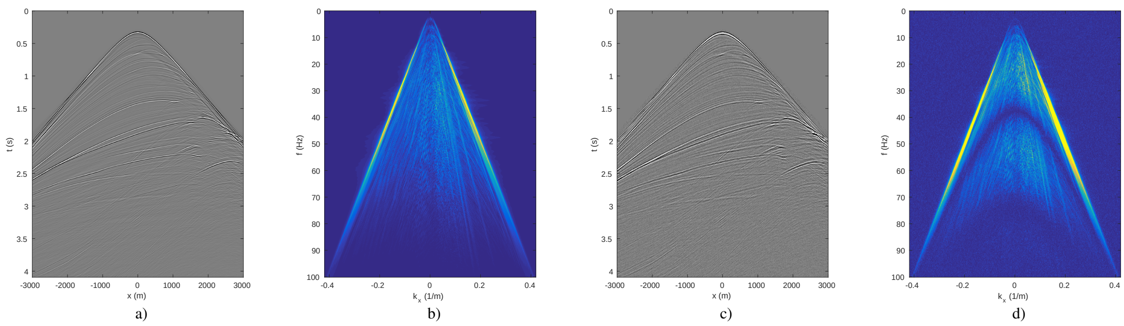

Figure 1 *a) Modelled shot record b) Modelled shot record in f-k domain c) Modelled shot record including ghost and noise d) Modelled shot record including ghost and noise in f-k domain)*

Figure 2 shows the estimated ghost-free data for the following methods: non-causal, closed-loop, sparse closed-loop, hybrid (non-causal/sparse closed-loop) and stabilized sparse closed-loop. The left-column

f-k spectra (Figure 2a) show the deghosted results for the input shot record of Figure 1c and d. The second-column f-k spectra, (Figure 2b, are the residuals with respect to the true ghost-free result (which is known in our case). In addition, the *signal* part of the input data is separately analysed for each method. The third-column f-k spectra, Figure 2c, shows the results. To get these, the signal was processed in exactly the same way as the signal-plus-noise. This could be realized by carrying out the processing of the signal parallel to the processing of the signal-plus-noise, and guiding the former by the latter. The spectra shown in the fourth column, Figure 2d, are the difference between the results shown in Figure 2c and the true ghost-free record. These results indicate that outside the notch area each method is quite accurate. The closed-loop method is most accurate with respect to signal reconstruction: it has the smallest residual in Figure 2d. On the other hand, in the notch areas the residual of the closed-loop method is quite high, see figure 2b. The other methods better balance between signal reconstruction and noise suppression. Looking at both residuals (columns 2 and 4) the sparse closed-loop method has the smallest total residual, especially if we focus on the first notch (at 0 Hz). In order to quantity the noise behaviour of the methods, the noise is separated from the signal in the deghosted results (i.e., the results in Figure 2c are subtracted from those in Figure 2a, resulting in $\mathbf{N}$). The obtained results were used to compute measures for signal reconstruction and noise (Table 1). The second column in Table 1 is the measure for signal reconstruction based on the estimated noise-free, deghosted data $\hat{\mathbf{P}}_0$ and true ghost-free data $\mathbf{P}_0$. The third column shows the noise level based on $\mathbf{N}$ and $\mathbf{P}_0$.

Table 1 *Table to quantify the performance of deghosting methods (first column) with respect to reconstructing signal (second column) and suppressing noise (last column).*

Deghosting Method	$10log(\frac{\hat{\mathbf{P}}_0-\mathbf{P}_0}{\mathbf{P}_0})^2$	$10log(\frac{\mathbf{N}}{\mathbf{P}_0})^2$
Closed-loop	-60.1 dB	-6.8 dB
Non-Causal	-40.3 dB	-16.4 dB
Sparse Closed-loop	-40.4 dB	-19.7 dB
Hybrid (Non-Causal+Sparse Closed-loop)	-44.1 dB	-17.7 dB
Stabilized Sparse Closed-loop	-48.4 dB	-17.1dB

Conclusions and Discussion

The deghosting process affects the SNR if noise is present in the data. Therefore, any deghosting method must be designed in such a way that the noise is controlled. Both the non-causal method and the closed-loop methods are capable of balancing between signal reconstruction and noise suppression. Separate measures for signal reconstruction and noise suppression were computed in the synthetic example. In this particular case the stabilized sparse closed-loop method delivered the most accurate result with respect to these two measures. More research is needed to determine what the effect is of a different SNR and other types of noise. Another approach that is interesting to compare is to apply a cascaded approach of a dedicated noise removal method followed by closed-loop deghosting.

Acknowledgements

The authors would like to thank the sponsors of the Delphi Research Consortium for their support.

References

Berkhout, A.J. [1985] *Seismic migration, imaging of acoustic energy by wave field extrapolation, A: theoretical aspects*. Elsevier (third edition).

Berkhout, A.J. and Blacquière, G. [2016] On the enhancement of low frequencies in marine seismic data. *86th SEG Conference & Exhibition*, Expanded abstracts, 162–167.

Orji, O.C., Sollner, W. and Gelius, L.J. [2013] Sea Surface Reflection Coefficient Estimation. *83rd SEG Conference & Meeting*, Expanded abstracts, 2150–2153.

Rickett, J., Manen, D.J.V., Loganathan, P. and Seymour, N. [2014] Slanted-streamer data-adaptive deghosting with local plane waves. *76th EAGE Conference & Meeting*, Extended abstracts, ELI1 15.

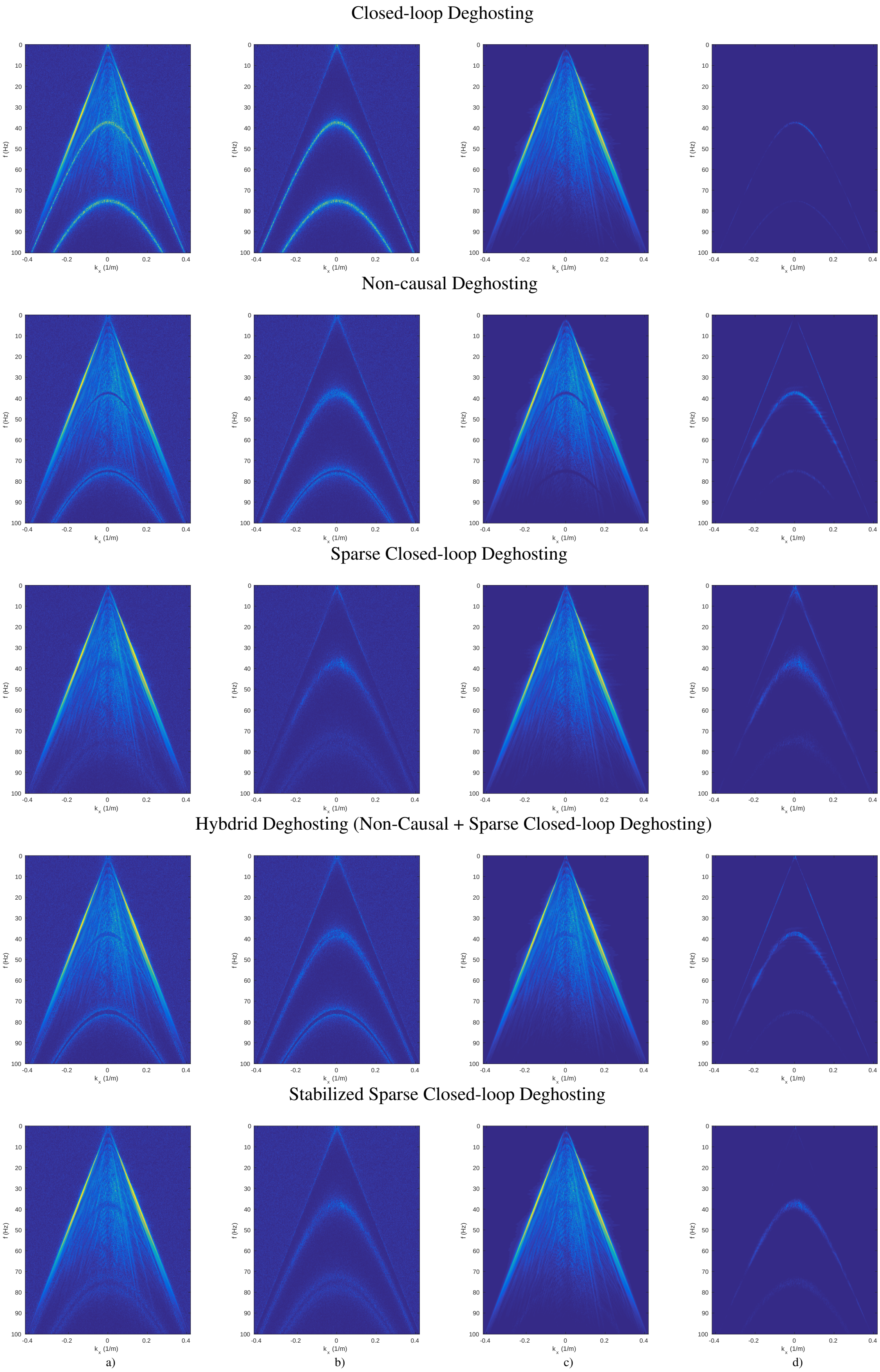

Figure 2 *Results are illustrated in the f-k domain. a) Deghosted shot record including noise b) Residual between deghosted record including noise and ghost-free record c) Deghosted record excluding noise d) Residual between deghosted record excluding noise and ghost-free record.)*